EFFECT OF CARBONATION ON PROPERTIES OF ALKALI-ACTIVATED SLAG BINDERS

JUAN HE [1] *, YONGHUA WU [1], CHANGHUI YANG [2], QIE GAO[1], XIAOLIN PU[1]
[1] College of Materials and Mineral Resources, Xi'an University of Architecture and Technology, Xi'an, China;
[2] College of Materials Science and Engineering, Chongqing University, Chongqing,China

AAS binders activated by water glass (WG) and sodium hydroxide (NaOH) solution was used to investigate its carbonation properties. Carbonation product, carbonation shrinkage, and effect of carbonation on pore structure of AAS paste were studied. Compared with noncarbonated one, when AAS paste was carbonated, specific surface area and cumulative pore volume increased, and average pore diameter and most probable pore diameter reduced. As for carbonation product, the main form of $CaCO_3$ is calcite, and the phases as vaterite and aragonite are lesser. The amount of aragonite and vaterite increases with the increase of carbonation age. During carbonation, the shrinkage only comes from the migration of Ca^{2+} from C-A-S-H gel and the increase of degree of polymerization (DP) of C-A-S-H gel. Carbonation process of AAS paste doesn't increase the dry shrinkage.

Keywords: Alkali-Activated Slag; Carbonation; Pore structure; Carbonation product; Carbonation shrinkage

1. Introduction

Researchers have a great interest in alkali-activated slag (AAS) binders due to their manufacturing process. With respect to ordinary Portland cement (OPC), an AAS binder has important benefits regarding the lower costs, energy and CO_2 emissions [1-4]. In addition, several studies indicate that AAS cements and concretes present excellent properties [5-8]. Nevertheless, previous research [9-12] has shown that AAS mortars and concretes are subject to substantial carbonation rate, which are one of the main drawbacks to the definitive use of AAS. And the behavior to carbonation has not yet fully explained.

As we know, the major hydration products of ordinary Portland cement (OPC) are calcium silicate hydrate (C-S-H) and portlandite (Ca(OH)$_2$). In general, carbonation of OPC concrete is the reaction of the dissolved CO_2 and Ca(OH)$_2$. In case of severe carbonation, the carbonic acid may react with the C-S-H gel and also with the yet unhydrated C_3S and C_2S, forming the main carbonation products of $CaCO_3$ and silica gel [13-15]. There is no portlandite (Ca(OH)$_2$) formed in hydration of AAS[16-19], therefore the carbonation mechanism in OPC and AAS systems is different.

Palacios and Puertas [10] studied the carbonation of AAS and OPC pastes. The authors observed that after carbonation, carbonate precipitation is much more intense in OPC than in AAS.

The authors attributed this to the fact that in Portland cement paste both the portlandite and the C-S-H gel can be carbonated, whereas in alkali-activated slag pastes, only the C-(A)-S-H gel is carbonated directly. Palacios and Puertas [20] also studied the carbonation of AAS and OPC mortars. AAS mortars were more intensely and deeply carbonated than OPC mortars. In Portland cement mortars, the precipitation of $CaCO_3$ in the matrix covers the pores and prevents more CO_2 to penetrate any deeper into the mortar. This, in conjunction with ongoing hydration, yields a denser and more compact mortar, which also increases the mechanical strength. When WG was used as the activator, after carbonation, cohesion in the matrix decreased, porosity increased and mechanical strength decreased. While in NaOH activated AAS mortars, carbonation enhanced the compaction and increased the mechanical strength, these mortars showing similar mechanical strength development like OPC mortars. A slight carbonation was observed in OPC mortar. While up to 10 mm carbonated front was recorded in WG-activated mortar and only 3 mm was recorded in NaOH-activated mortar.

Bakharev et al.[9] prepared AAS concrete activated with liquid sodium silicate (SiO$_2$/ Na$_2$O ratio of 0.75).They found that AAS concrete carbonated more serious than OPC concrete, and

---

AAS concrete showed higher strength loss than OPC concrete. Bernal et al. [21] studied the carbonation characteristics of alkali-activated (AA) metakaolin (MK) and slag blends. They achieved that as carbonation proceeds, compressive strength decreases roughly linearly. Also, Bernal et al. [22] studied AA fly ash (FA) and slag blends. The results indicate that carbonation caused a high polymerised alumina-silicate gel in AA slag in which C-A-S-H gel formed. While in AA FA, N-A-S-H gel formed.

In general, AAS mortars and concretes suffer more severe carbonation than OPC mortars and concretes. After carbonation, in comparison with OPC, AAS mortars and concretes have higher strength loss. The type and content of slag activator and solution modulus all affect the carbonation process and products. However, there have been very limited works performed on the effect of carbonation on the microstructure of AAS paste. In particular, detailed investigation of the evolution of the carbonation products is needed to elucidate.

Therefore, in this paper, AAS binders activated with WG and sodium hydroxide (NaOH) solution were used to investigate the effect of carbonation on the shrinkage behavior. The products of carbonation and the DP change of C-A-S-H gel were identified by FT-IR analysis. Also the effect of carbonation on the pore structure of AAS hardened pastes were analysed by using nitrogen absorption measurement.

2. Experimental

2.1. Materials

Slag used in this study came from Chongqing Steel and Iron Group. The blast-furnace slag is a granulated product ground to fineness of about 453 m^2/kg, with the main particle size lesser than 25 μm. The basicity coefficient (K_b= (CaO +MgO)/(SiO_2+Al_2O_3)) of slag equals to 1.07 and the density is 2.85g/cm^3.

Ordinary Portland cement (OPC) was used as a reference. OPC was prepared by grinding clinker (Chongqing Lafaji Rui An Cement Co., Ltd.)

with 4% gypsum. The fineness of OPC clinker was 406 m^2/kg and its density was 3.22 g/cm^3. The chemical compositions of slag and OPC are shown in Table 1. AAS binders were prepared by using WG and sodium hydroxide (NaOH) solutions (30% concentration) as activators. WG is an industrial product and its chemical composition is shown in Table 2. Sodium hydroxide (NaOH) is caustic soda flake from Deyang, Sichuan. NaOH was blended with WG to adjust the modulus (Ms) of WG solution (molar ratio of SiO_2 to Na_2O) to be 1.0, 1.2, 1.5, 1.8 and 2.0 respectively.

2.2. Experimental procedures

The water/binder ratio of cement pastes was 0.30 and the Na_2O alkali equivalent was 4%. W1.0, W1.2, W1.5, W1.8 and W2.0 indicated that the modulus of activator were 1.0, 1.2, 1.5, 1.8, 2.0 respectively. N4 indicated the sample of AAS paste activated with NaOH. And the OPC was the ordinary Portland cement sample. The pastes were cast in small cylindrical plastic molds with the size of φ27.5mm×50mm. The specimens were cured in the standard-curing room at relative humidity (RH) of 95% and 20 ℃ for 1 day and then demolded. Subsequently the specimens were cured in the standard-curing room (approximately the same conditions) until the testing date.

2.2.1. Accelerated carbonation test

After 27 days of curing in standard conditions, the AAS specimens were moved into dry shrinkage chamber (with temperature of 20℃ and relative humidity 70%) for 24 hours. After that, the circumference surface and one bottom of specimens were both coated with wax, and only another bottom surfaces were exposed to the accelerated carbonation environment into carbonation chamber. The temperature and relative humidity in this chamber were controlled at 20±1℃ and 70±5%, respectively. CO_2 concentration in this chamber was 20±3%. At the testing date (3 days, 7 days, 14 days, 28 days and 60 days), the specimens were split along the surface with no wax and cleaned, and then the freshly broken surfaces were sprayed with 1% of

Table 1

Chemical compositions of slag and OPC clinker

	SiO_2(%)	Al_2O_3(%)	CaO(%)	Fe_2O_3(%)	MgO(%)	SO_3(%)	K_2O(%)	Na_2O(%)	Loss of ignition(%)
Slag	30.97	11.40	37.59	1.79	7.60	0.22	0.66	0.37	1.01
OPC clinker	20.20	5.89	63.60	3.92	1.46	--	0.34	0.18	1.55

Table 2

Chemical composition and physical properties of WG

SiO_2(%)	Na_2O(%)	Ms	Baume degree(°Bé)	Density(g/cm^3)
26.49	9.95	2.75	40.0	1.405

phenolphthalein in the solution of absolute ethyl alcohol. The carbonated portion is uncolored and non-carbonated portion is purple.

2.2.2. Pore structure

After 28 days of standard curing or 28 days carbonation, the specimens were broken into pieces of 1-2cm, and then they were dried for 24 hours at 60℃ in vacuum drying chamber. Afterwards, they were cooled slowly to room temperature to be ready to study of pore structure. The carbonated portion (no color portion with phenolphthalein solution) in carbonated specimens should be chosen for the test. Pore structure was carried out using an ASAP2020 specific surface area and pore analyzer of Micromeritics Instrument Corp. Nitrogen is used as adsorbent gas. The adsorption and desorption time was 8 hours, and the desorption temperature was 110℃.

2.2.3. Carbonation products

The products of carbonation and their microscopic structure were identified by FT-IR analysis. A Nicolet 5DXC for FTIR spectroscopy was used. KBr slices (1.0 mg of sample to 300 mg of KBr) were prepared. Frequencies were scanned across a range of 4000-400 cm^{-1}.

2.2.4. Shrinkage of cement paste specimens

The volume deformation under no load is mostly isotropic, so linear variation of the diameter of cement paste specimens was used to characterize their volume change, namely diameter change rate. After standard cured for 27 days, the paste cylinders were cut into 1-mm thick discs. Then the discs were placed in dry shrinkage chamber (temperature 20±1℃ and relative humidity 70±5%) for 1 days. Subsequently, disc diameter in three directions (120 angles included) was measured using a vernier caliper. That is the initial diameter. then half of the discs were placed in carbonation chamber, and the other half of the discs were placed in another chamber, at constant temperature and humidity - the same conditions as carbonation chamber (20±1℃, RH=70±5%). At testing age, disc diameters of paste specimens cured in chamber with constant temperature and humidity (dry shrinkage conditions) and in carbonation chamber were measured respectively, then the diameter change rate (d,%) were calculated by

$$d = \sum_{j=1}^{3}(\sum_{i=1}^{3}\frac{D_i-D_{i0}}{D_{i0}}/3)/3 \times 100\% \qquad (1)$$

Where D_{i0} is the initial disc diameter i of sample j (mm). D_i is the disc diameter i of sample j at the testing age (mm).

Diameter change rate of dry shrinkage and carbonation shrinkage are expressed as d1 and d2 respectively. The carbonation shrinkage under this condition is a comprehensive reflection of the

volume change of cement paste attributed to drying and carbonation.

3. Results and discussions

3.1 Effect of carbonation on the pore structure

3.1.1. Isothermal adsorption and desorption curve

Figure 1 presents the isothermal adsorption and desorption curve of AAS pastes activated with WG and NaOH solution. The isothermal adsorption curves were not consistent with the desorption curves, causing the hysteresis loop. In the process of adsorption, at low pressure, nitrogen first condenses in small diameter pores. When nitrogen pressure increases gradually, nitrogen also condenses in big diameter pores, until it reaches the saturation pressure, condensation in the flat part of the pore occurs.
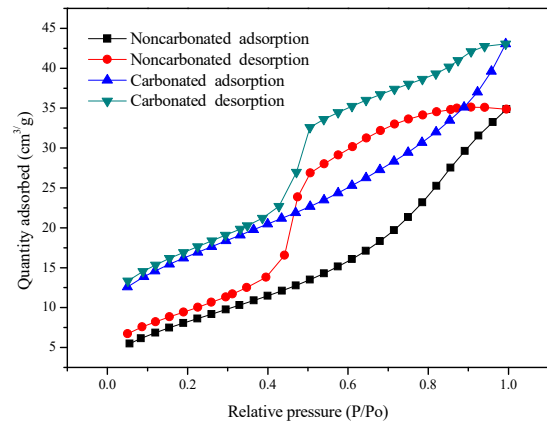
(a) AAS paste with WG（W1.0）
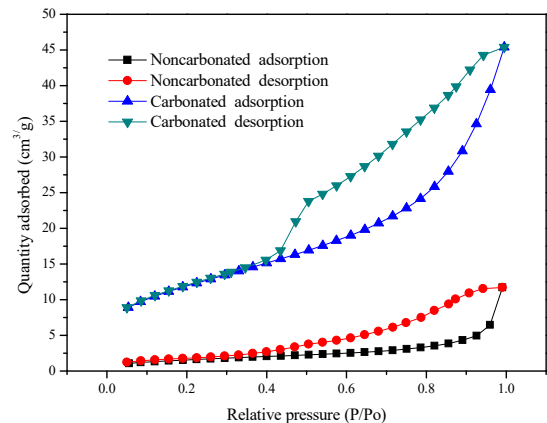
(b) AAS paste with NH (N4)

Fig.1 - Isothermal adsorption-desorption curves of AAS pastes.

Isothermal adsorption curves of WG-activated AAS paste of noncarbonated and carbonated specimens were approximately parallel and the carbonated adsorption curves were above the noncarbonated one. This shows that at the same pressure, carbonated paste adsorbs more nitrogen. So it can be qualitatively judged that the content of small diameter pores increases after carbonation for WG-activated AAS paste (Fig. 1a). While for NaOH-activated AAS paste, isothermal

Specific surface area and pore structure parameter of hardened cement pastes

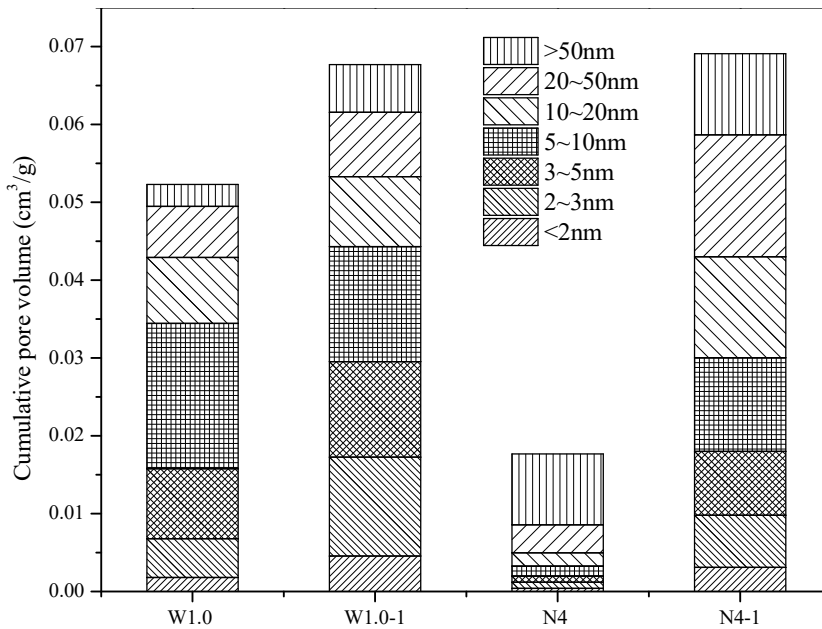| Item	W1.0		N4	
	Noncarbonated	Carbonated	Noncarbonated	Carbonated
BET surface area (m^2/g)	31.7515	57.3852	5.8459	42.4493
Average pore diameter (nm)	5.8892	4.8585	12.9771	6.8721
Cumulative pore volume (cm^3/g)	0.0523	0.0677	0.0176	0.0691
Most probable pore diameter (nm)	7.4827	2.2985	57.1749	15.9476

Fig. 2 - Pores distribution of some AAS pastes

Note: W1.0 and N4 are specimens of 28 days standard curing; W1.0-1 and N4-1 are specimens of 28 days carbonation.

adsorption-desorption curves of noncarbonated and carbonated specimens was very different (Fig. 1b). The curve of noncarbonated paste was completely below the curve of carbonated, and the nitrogen adsorption quantity was quite different. The nitrogen adsorption quantity of the former was quite smaller than the latter. This shows that pore structure appears great change after carbonation. It can be qualitatively judged that after carbonation, the content of pores, especially the small diameter pore increases greatly. This also shows that carbonation of NaOH-activated AAS paste has a bigger effect on the pore structure than WG-activated AAS paste. Besides, for noncarbonated AAS paste, compared with WG-activated AAS paste, nitrogen adsorption quantity of NaOH-activated AAS paste was quite smaller, so the pore structure is quite different, and the small diameter pore is probably much lesser.

3.1.2. Pore structure analysis of AAS paste

Adsorption curve data of the adsorption isotherms curves was used to analyze the specific surface area and pores structure parameter of AAS paste. The results are shown in Table 3 and Figure 2. Table 3 shows that for noncarbonated AAS activated with WG, specific surface area and cumulative pore volume are greater compared with NaOH-activated AAS paste, and a smaller average pore diameter and most probable pore diameter.

In addition, when AAS paste was carbonated, specific surface area and cumulative pore volume increased, and average pore diameter and most probable pore diameter reduced, in comparison with noncarbonated one. When WG was used as activator, cumulative pore volume increased since 0.0523 cm^3/g to 0.0677 cm^3/g. When NaOH was used as activator, cumulative pore volume increased since 0.0176 cm^3/g to 0.0691 cm^3/g. The increase of the former is much smaller than the latter.

Carbonation process consumes Ca^{2+} in pore solution, and the ion balance of pore solution is broken. $Ca(OH)_2$ doesn't exist in the hydration products of AAS paste, so C-A-S-H gel decalcifies to keep the balance of Ca^{2+} in pore solution. C-A-S-H gel converts into a high polymerization and low Ca/Si gel. C-A-S-H gel of high density converts into C-A-S-H gel of low density. The precipitation of carbonation product - $CaCO_3$ in capillary pore divides large diameter pores into small ones. Therefore, after carbonation, specific surface area and cumulative pore volume of AAS paste increase [23, 24], while average pore diameter and most probable pore diameter reduce [25, 26].

Figure 2 shows the pores distribution of some AAS pastes. For noncarbonated AAS paste, when WG was used as activator, small diameter pores (≤ 20nm) were much more than large diameter pores. The cumulative volume of pores

with diameter smaller than 20 nm was 0.0429 cm³/g, meaning 82.1% of the total cumulative pore volume. Therefore, its specific surface area is large, and average pore diameter and most probable pore diameter are small. When NaOH was used as activator, small diameter pores were much less than large diameter pores. The cumulative pore volume of pores with diameter larger than 20 nm was 0.0127 cm³/g, meaning 72.2% of the total cumulative pore volume. Therefore, its specific surface area is small, and average pore diameter and most probable pore diameter are large. Besides, for NaOH-activated AAS paste, there was much more pores with diameter larger than 50 nm. That in favour of the diffusion of CO_2 in AAS paste, determining a great carbonation. Water loss from pores of AAS paste also causes much shrinkage.

For carbonated AAS paste, when WG was used as activator, all pores increased, excepting the pores between 5-10nm which reduced. In NaOH-activated binder, pores of all diameteres increased after carbonation. Especially the pores smaller than 50nm increased much more, and the pores larger than 50nm increased much less. So after carbonation, specific surface area increased, and the average pore diameter and most probable

pore diameter decreased. Puertas used NaOH to prepare AAS mortar. Also, his test results show that the average pore diameter decreases after carbonation [20].

3.2. FT-IR analysis of carbonation product of AAS paste

Figures 3-5 show the IR spectra of AAS paste after standard-curing and carbonation. The IR spectra of hydration and carbonation products are relative similarly. The absorption peaks around 3445cm⁻¹ are caused by the stretching vibration of OH⁻, and the absorption peaks at about 1640 cm⁻¹ are caused by the flexural vibration of OH⁻[27].

The stretching vibration of OH⁻ in Ca(OH)₂ is at about 3635cm⁻¹, which is not appeared in all hydration product spectra. This indicates that there is no Ca(OH)₂ in the hydration products. A broad and large absorption peak appears at about 958cm⁻¹-977cm⁻¹.That suggests the presence of $Si_2O_7^{6-}$ groups in C-A-S-H gel of hydration product. The degree of polymerization (DP) of $[Si_2O_7]^{6-}$ groups is 2, and some of the Si^{4+} is replaced by Al^{3+} in $[Si_2O_7]^{6-}$ group. This peak about 958cm⁻¹-977cm⁻¹ is caused by an asymmetric stretching vibration of Si-O or Al-O.
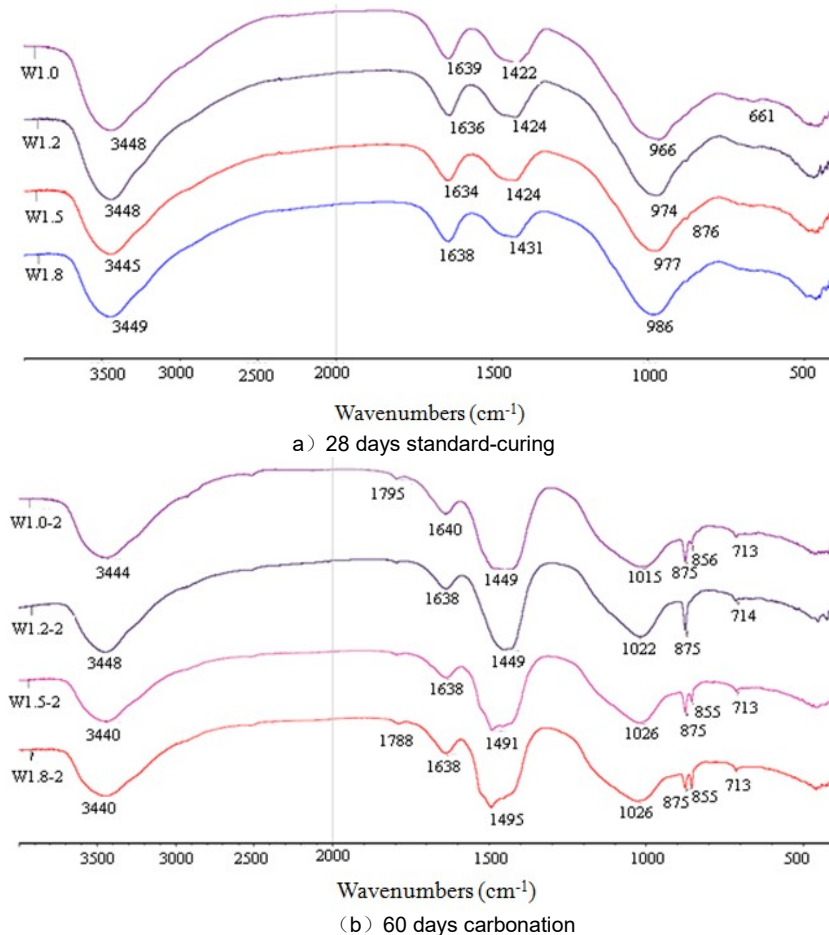

a）28 days standard-curing

（b）60 days carbonation

Fig.3 - IR spectra of AAS paste activated with WG after 28 days curing and 60 days carbonation

Note：W1.0, W1.2, W1.5 and W1.8 are specimens of 28 days standard curing；W1.0-2, W1.2-2, W1.5-2 and W1.8-2 are specimens of 60 days carbonation.
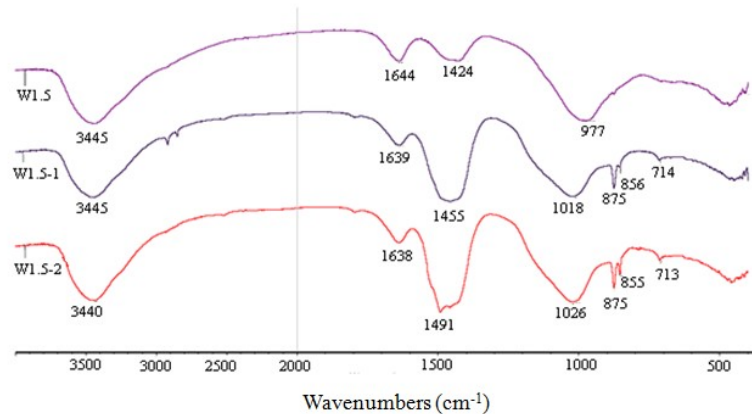
Fig.4 - IR spectra of AAS paste activated with WG after 28 days standard-curing and 28 days and 60 days carbonation
Note: W1.5, W1.5-1 and W1.5-2 are specimens of 28 days standard curing, 28 days carbonation and 60 days carbonation respectively.
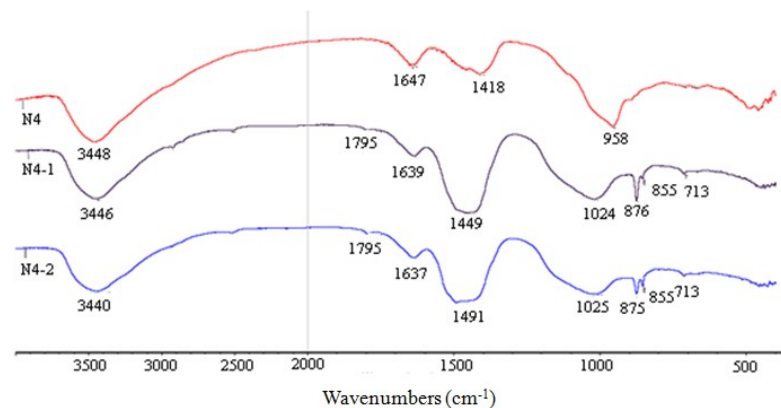

Fig.5 - IR spectra of AAS paste activated with NaOH after 28 days curing, 28 days and 60 days carbonation
Note: N4, N4-1 and N4-2 are specimens of 28 days standard curing, 28 days carbonation and 60 days carbonation respectively.

Compared with the noncarbonated one, after carbonation, the absorption peak of 1418 cm^{-1}-1431cm^{-1} moves to the higher wave number of 1449 cm^{-1}-1495 cm^{-1}. And peaks become narrower and higher. The absorption peak of 958 cm^{-1}-986 cm^{-1} disappears, and the absorption peak of higher wave number of 1015 cm^{-1}-1026cm^{-1} appears. Also, the absorption peaks of wave number of 1795 cm^{-1}, 875cm^{-1}, 855cm^{-1}, and 713cm^{-1} appear.

The absorption peaks of wave number 1449 cm^{-1}-1495 cm^{-1}, 1795 cm^{-1}, 875 cm^{-1}, 855 cm^{-1} and 713 cm^{-1} represent a typical feature of $[CO_3]^{2-}$. Peaks of 1449 cm^{-1}-1495 cm^{-1} becoming narrower and higher indicates the $[CO_3]^{2-}$ content increases. The absorption peak of 875cm^{-1}, 855cm^{-1}, and 713cm^{-1} are caused by the flexural vibration of $[CO_3]^{2-}$. The most notable difference between calcite and aragonite is the absorption peak with wave numbers of 875 cm^{-1} and 855 cm^{-1}. The 875 cm^{-1} is the characteristic peak of calcite, and the 855 cm^{-1} is the characteristic peak of aragonite. Except for W1.2-2 in Figure 3 (b), the absorption peak of 855cm^{-1} is quite clear in all carbonated AAS pastes. This indicates that some $CaCO_3$ exists in the form of aragonite. In comparison with carbonated specimen for 28days (Figures 4 and 5), in carbonated specimen for 60 days, the absorption peak of 855cm^{-1} become stronger. This

suggests that the amount of aragonite increases with the increase of carbonation age. In addition, in spectra of W1.5-2、W1.8-2 and N4-2, near to the absorption peak of 1490 cm^{-1}, there is also an absorption peak at about 1420 cm^{-1}.This is characteristic for vaterite. Therefore, three variants of calcium carbonate, which are calcite, aragonite and vaterite, all may exist in carbonated specimens. And the amount of aragonite and vaterite increases with the increase of carbonation age.

After carbonation, the absorption peak of 958 cm^{-1}-986 cm^{-1} moves to a higher wave number of 1015 cm^{-1}-1026 cm^{-1}. Also, the C-A-S-H gel rich in silicon is generated, and the DP of C-A-S-H gel increases.

3.3. Carbonation shrinkage

Figure 6 shows the diameter change rate as consequence of dry shrinkage and carbonation shrinkage. Before 28 days of carbonation, dry shrinkage and carbonation shrinkage increase much more, then it increases little. For AAS paste, its carbonation shrinkage is lesser than dry shrinkage. For OPC paste, the carbonation shrinkage is more than dry shrinkage. Carbonation degree of AAS paste doesn't increase the dry shrinkage, although carbonation degree of OPC
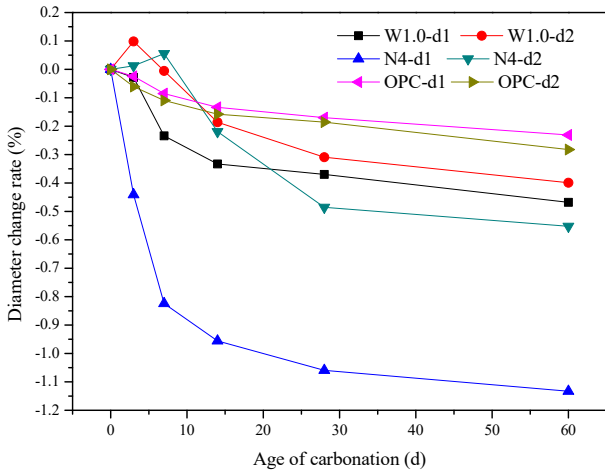
Fig.6 - Drying shrinkage and carbonation shrinkage of cement pastes

Note: W1.0-d1, N4-d1 and OPC-d1 are diameter change rate of dry shrinkage; W1.0-d2, N4-d2 and OPC-d2 are diameter change rate of carbonation shrinkage.

paste promotes the development of drying shrinkage.

Dry shrinkage decreases in following order: NaOH-AAS paste＞WG-AAS paste＞OPC paste. Effect of carbonation on dry shrinkage of AAS and OPC paste is different. During the initial stage of carbonation, diameter of AAS paste increases slightly, then with the carbonation process progress, the diameter continuously decreases and stabilizes. For OPC paste, the diameter of specimen decreases continuously in parallels with the carbonation process.

C-S-H gel with high Ca/Si ratio and crystalline $Ca(OH)_2$ are the main hydration products of OPC. The $Ca(OH)_2$ deforms small when ambient humidity changes. The deformation of C-S-H gel with the variation of ambient humidity is much bigger [28-29]. The authors agree that the existence of $Ca(OH)_2$ crystal is the main reason for the small drying shrinkage of OPC paste.

In AAS hydration products there is no exist crystalline $Ca(OH)_2$ and the main hydration products is C-A-S-H gel. This is the main cause of large dry shrinkage of AAS. Besides this, in AAS paste there are smaller diameter pores. Based on the theory of capillary tension, the smaller the pores, the larger the shrinkage stress is, and the greater the shrinkage is. There are more pores having the diameter larger than 50nm in NaOH-activated AAS paste (see Fig. 2). Meanwhile, under the experimental conditions (RH=(70±5) %), dry shrinkage due to water loss from pores larger than 50nm is the main cause, for larger dry shrinkage of NaOH-activated AAS paste in comparison with WG- activated AAS paste.

During the initial stage of carbonation, consumption of Ca^{2+} in pore solution of OPC paste is compensated by dissolution of solid $Ca(OH)_2$. According to the above analysis, the dissolution of $Ca(OH)_2$ loses the role to prevent the deformation

of lost C-S-H gel, and increases the small pores. So the C-S-H gel is more sensitive to deformation by dry shrinkage. With the further carbonation, C-S-H gel decalcifies, and its DP increases, causing new shrinkage. Therefore, carbonation shrinkage of OPC paste is caused mainly by two aspects. One is the dissolution of solid $Ca(OH)_2$, the other is the decalcification of C-S-H gel and the increase of its DP. In OPC paste, shrinkage coming from carbonation is stronger than prohibiting shrinkage coming from the precipitation of $CaCO_3$. When carbonation occurred, shrinkage increased. Therefore, specimen diameter of OPC paste decreases continuously.

There is no $Ca(OH)_2$ crystal exist in AAS hydration products, so there is no shrinkage coming from the dissolution of solid $Ca(OH)_2$. The shrinkage comes only by the migration of Ca^{2+} from C-A-S-H gel and the increase of its DP. So, carbonation shrinkage in AAS paste is smaller in comparison. The precipitation of carbonation products in pores increases the compactness and the resistance to deformation of AAS paste, inhibiting the shrinkage of this. In AAS paste, prohibiting shrinkage coming by carbonation is stronger than the increase of shrinkage. So after carbonation, shrinkage of AAS paste reduces.

Figure 6 also shows that at the initial stage of carbonation, there is no reduction in specimen diameter of AAS paste, even there is some increase. That is to say, there is no shrinkage but expansion. There is more Na^+ and K^+ content, while very low Ca^{2+} content in pore solution. CO_3^{2-} reacts with Na^+, K^+ and Ca^{2+} to form Na_2CO_3, K_2CO_3 and $CaCO_3$. So, Na^+, K^+ and Ca^{2+} absorb the CO_2, hindering the decalcification of C-A-S-H gel. When the concentration of Na_2CO_3, K_2CO_3 and $CaCO_3$ reaches supersaturation, the crystal phase form and the AAS paste shows swelling properties. With the continuous carbonation process, the migration of Ca^{2+} from C-A-S-H gel and absorbtion of CO_2 is the main reaction, so the shrinkage due to the decalcification becomes strong. Specimen diameter of AAS paste decreases until becomes stable. This also needs further in-depth study.

4. Conclusions

1. Compared with noncarbonated one, when AAS paste was carbonated, specific surface area and cumulative pore volume increased, and average pore diameter and most probable pore diameter reduced.
2. Three variants of calcium carbonate, which is calcite, aragonite and vaterite, all may exist in carbonated specimens. The amount of aragonite and vaterite increases with the increase of carbonation age. After carbonation, the C-A-S-H gel rich in silicon is generated, and its DP increases.

3. During carbonation, for AAS hardened pastes there is no shrinkage coming from the dissolution of solid $Ca(OH)_2$. The shrinkage comes only by the migration of Ca^{2+} from C-A-S-H gel and the increase of its DP. Carbonation degree of AAS paste doesn't increase the dry shrinkage.

REFERENCES

1. D. M. Roy, Alkali-activated cements Opportunities and challenges, Cement and Concrete Research, 1999, **29**, 249.
2. J. L. Provis, A. Palomo, C. J. Shi, Advances in understanding alkali-activated materials, Cement and Concrete Research, 2015, **78,** 110.
3. M. R. Alaa, A comprehensive overview about the influence of different additives on the properties of alkali-activated slag-A guide for Civil Engineer, Construction and Building Materials, 2013, **47**, 29.
4. M. Torres-Carrasco, F. Puertas, Alkaline activation of aluminosilicates as an alternative to Portland cement: a review, Romanian Journal of Materials 2017, **47** (1), 3.
5. M.M. Alonso, S. Gismera, M.T. Blanco, et al., Alkali-activated mortars: Workability and rheological behavior, Construction and Building Materials, 2017,**145**,576.
6. A. M. Moncea, M. Georgescu, A. Melinescu, et al., Hardening processes and hydrates in alkali-activated slag and geopolymer with Pb content, Romanian Journal of Materials, 2012, **42**, 356.
7. T.Bakharev, J. G. Sanjayan, Y. B. Cheng, Resistance of alkali-activated slag concrete to acid attack, Cement and Concrete Research, 2003, **33**, 1607.
8. M. M. Hossain, M. R.Karim, M. K. Hossain, et al., Durability of mortar and concrete containing alkali-activated binder with pozzolans: A review, Construction and Building Materials, 2015, **93**, 95.
9. T. Bakharev, J. G. Sanjayan, Y. B. Cheng, Resistance of alkali-activated slag concrete to carbonation, Cement and Concrete Research, 2001, **31**, 1277.
10. M. Palacios, F. Puertas, Effect of carbonation on alkali-activated slag paste, Journal of the American Ceramic Society, 2006,**89**,3211.
11. S. Al-Otaibi, Durability of concrete incorporating GGBS activated by water-glass, Construction and Building Materials, 2008, **22**, 2059.
12. S. A.Bernal, R. M.de Gutierrez, J.L. Provis, et al., Effect of silicate modulus and metakaolin incorporation on the carbonation of alkali silicate-activated slags, Cement and Concrete Research, 2010**, 40**, 898.
13. J. Z. Liu JZ, A review of carbonation in reinforced concrete (I): Mechanism of carbonation and evaluative methods, Concrete, 2005, **11**, 10. (in Chinese)
14. J. He, C.H.Yang, Analysis of Carbonation on Portland Cement Concrete, Bulletin of the Chinese Ceramic Society, 2009, **28**, 1225.
15. S. Alexander, D. Dieter, A. Hermann, Modeling carbonation for corrosion risk prediction of concrete structures, Cement and Concrete Research, 2002, **32**, 935.
16. S. D. Wang, K. L. Scrivener, Hydration products of alkali activated slag cement, Cement and Concrete Research, 1995, **25**,561.
17. I. G. Richardson, A. R. Brough, G. W. Groves, et al., The characterization of hardened alkali-activated blast-furnace slag paste and the nature of the calcium silicate hydrate (C-S-H), Cement and Concrete Research, 1994, **24**,813.
18. P. T. Fernando, C. G. João, J. Said, Alkali-activated binders: A review Part 1. Historical background, terminology, reaction mechanisms and hydration product, Construction and Building Materials, 2008, **22**, 1305.
19. P. T. Fernando, C. G. João, J. Said, Alkali-activated binders: A review. Part 2. About materials and binders manufacture, Construction and Building Materials, 2008, **22**, 1315.
20. F. Puertas, M. Palacios, T. Vázquez, Carbonation process of alkali-activated slag mortars, Journal of Materials Science, 2006, **41**, 3071.
21. S.A.Bernal, R.M.D. Gutiérrez, J.L. Provis, Engineering and durability properties of concretes based on alkali-activated granulated blast furnace slag/metakaolin blends, Construction and Building Materials, 2012, **33**, 99.
22. S. A. Bernal, J.L. Provis, B. Walkley, et al., Gel nanostructure in alkali-activated binders based on slag and fly ash, and effects of accelerated carbonation. Cement and Concrete Research, 2013, **53**, 127.
23. J. J. Thomas, J. J. Chen, A. J. Allen, et al., Effects of decalcification on the microstructure and surface area of cement and tricalcium silicate pastes, Cement and Concrete Research,2004, **34**, 2297.
24. P. D. Tennis, H. M. Jennings, (2000) A model for two types of calcium silicate hydrate in the microstructure of Portland cement pastes, Cement and Concrete Research, 2000, **30**, 855.
25. Y. H. Fang, Y. T. Zhang, X. Y. Mo, et al., Influence of carbonation on the microstructure and permeability of hardened cement paste and mortar, Journal of Hohai University:Natural Sciences, 2005,**33**, 104. (in Chinese)
26. V. T. Ngala, C. L. Page, Effect of carbonation on pore structure and diffusional properties of hydrated cement pastes, Cement and Concrete Research, 1997, **27**, 995.
27. W. Mozgawa, J. Deja, Spectroscopic studies of alkaline activated slag geopolymers, Journal of Molecular Structure,2009, **924-926**,434.
28. J. J.Thomas, H. M. Jennings, (2003) Changes in the Size of Pores During Shrinkage (or Expansion) of Cement Paste and Concrete, Cement and Concrete Research, 2003, **33**, 1897.
29. C. J. Wan, H. M. Jennings, J. J. Thomas, et al., The shrinkage behavior of decalcified cement paste, 12th international congress on the chemistry of cement. Montreal, Canada, 2007, July 8-13.

****